

RESEARCH ARTICLE

10.1002/2017JA024805

Key Points:

- A clear strong linear dependence of phase scintillation index on the plasma drift speed around noon sector of the polar ionosphere is presented
- Observed dependence can be very possibly explained by the dependence of the shifted Fresnel frequency from the relative drift
- Amplifies the importance of using dynamic cutoff frequency in detrending the phase of GPS signal in the polar region

Correspondence to:

Q.-H. Zhang and Z.-Y. Xing,
zhangqinghe@sdu.edu.cn;
xingzanyang@sdu.edu.cn

Citation:

Wang, Y., Zhang, Q.-H., Jayachandran, P. T., Moen, J., Xing, Z.-Y., Chadwick, R., et al. (2018). Experimental evidence on the dependence of the standard GPS phase scintillation index on the ionospheric plasma drift around noon sector of the polar ionosphere. *Journal of Geophysical Research: Space Physics*, 123, 2370–2378. <https://doi.org/10.1002/2017JA024805>






Received 21 SEP 2017

Accepted 6 MAR 2018

Accepted article online 8 MAR 2018

Published online 25 MAR 2018

Experimental Evidence on the Dependence of the Standard GPS Phase Scintillation Index on the Ionospheric Plasma Drift Around Noon Sector of the Polar Ionosphere

Y. Wang¹ , Q.-H. Zhang¹ , P. T. Jayachandran², J. Moen³, Z.-Y. Xing¹ , R. Chadwick², Y.-Z. Ma¹, J. M. Ruohoniemi⁴ , and M. Lester⁵ 

¹Shandong Provincial Key Laboratory of Optical Astronomy and Solar-Terrestrial Environment, Institute of Space Sciences, Shandong University, Weihai, China, ²Physics Department, University of New Brunswick, Fredericton, New Brunswick, Canada, ³Department of Physics, University of Oslo, Oslo, Norway, ⁴Bradley Department of Electrical and Computer Engineering, Virginia Tech, Blacksburg, VA, USA, ⁵Department of Physics and Astronomy, University of Leicester, Leicester, UK

Abstract First experimental proof of a clear and strong dependence of the standard phase scintillation index (σ_{ϕ}) derived using Global Positioning System measurements on the ionospheric plasma flow around the noon sector of polar ionosphere is presented. σ_{ϕ} shows a strong linear dependence on the plasma drift speed measured by the Super Dual Auroral Radar Network radars, whereas the amplitude scintillation index (S_4) does not. This observed dependence can be explained as a consequence of Fresnel frequency dependence of the relative drift and the used constant cutoff frequency (0.1 Hz) to detrend the data for obtaining standard σ_{ϕ} . The lack of dependence of S_4 on the drift speed possibly eliminates the plasma instability mechanism(s) involved as a cause of the dependence. These observations further confirm that the standard phase scintillation index is much more sensitive to plasma flow; therefore, utmost care must be taken when identifying phase scintillation (diffractive phase variations) from refractive (deterministic) phase variations, especially in the polar region where the ionospheric plasma drift is much larger than in equatorial and midlatitude regions.

1. Introduction

Any transionospheric radio signal encounters various effects such as group delay, phase advance, and random rapid fluctuations of the amplitude and phase of the signal, because of the presence of plasma and structures within the ionosphere. Most of these effects can be corrected or mitigated using multifrequency measurements. However, rapid and random fluctuations of amplitude and phase (scintillation) cannot be easily corrected or mitigated (Kintner et al., 2007). Under these conditions, Global Satellite Navigation System (GNSS) including Global Positioning System (GPS) signals are degraded or become completely useless. Phase variation in a transionospheric radio signal (e.g., GPS signal) can be broadly classified into two categories: (a) refractive (deterministic) which can be corrected using multifrequency measurements and (b) diffractive (stochastic), such as scintillations, which cannot be corrected. Historically, diffractive fluctuations (scintillation) in amplitude and phase are quantified by using the amplitude scintillation index (S_4 , normalized standard deviation of the amplitude for a 1 min interval) and the phase scintillation index (σ_{ϕ} , standard deviation during a 1 min period). In order to derive these scintillation indices using GNSS (such as GPS) measurements, a long-term trend needs to be removed, consisting of the Doppler shift due to the satellite receiver relative motion and slowly varying background ionosphere, and some hardware effects such as clock drift. A sixth-order Butterworth filter with a 0.1 Hz cutoff frequency in standard processing is often used to detrending the signal (e.g., Prikryl et al., 2014). This 0.1 Hz cutoff frequency was obtained statistically using wideband satellite measurements (Fremouw et al., 1978) and now widely used by many GPS receiver manufacturers and users for automated calculation of scintillation indices, which can be simply considered as the Fresnel frequency (e.g., Van Dierendonck & Arbesser-Rastburg, 2004; Van Dierendonck et al., 1993). If one does not choose this frequency carefully, the refractive variations will also be included (Forte & Radicella, 2002; Mushini et al., 2012), making phase scintillation index useless for the intended purpose in study of scintillation especially under the disturbed conditions. Many researchers have used these indices (as provided by the receiver), for scientific purposes including the identification of the scintillation formation mechanisms and space weather effects on GNSS signals (e.g., De Franceschi

et al., 2008; Moen et al., 2013; Oksavik et al., 2015; Prikryl et al., 2010, 2012, 2014). However, the Fresnel frequency linearly depends on the relative velocity between the receiver, the ionosphere, and the GPS satellite (e.g., Forte & Radicella, 2002). For equatorial and midlatitude regions, the ionospheric drift is typically around 100 m/s (e.g., Kintner et al., 2004) and the use of 0.1 Hz should be adequate. For high-latitude regions, however, it is an entirely different scenery because of the very high and variable ionospheric drift velocity (~ 100 m/s– $1,500$ m/s) (e.g., MacDougall & Jayachandran, 2001). The value of the cutoff frequency does not affect the determination of the amplitude scintillation index, but it does affect the phase scintillation index very much (Beach, 2006; Forte & Radicella, 2002; Mushini et al., 2012). The use of an inaccurate cutoff frequency also led to several cases of “phase without amplitude scintillation” event studies (e.g., Doherty et al., 2003; Li et al., 2010; Pi et al., 2001), showing phase scintillation occurrence much higher than the amplitude scintillation in the polar region (Jin et al., 2015; Prikryl et al., 2013; Spogli et al., 2009). Wavelet-based detrending methods have been adapted to address some of these issues (Materassi et al., 2009; Materassi & Mitchell, 2007; Mushini et al., 2012). To better represent phase scintillation, two new phase scintillation indices have been proposed, providing a more robust performance against detrending effects (e.g., Forte, 2005; Mushini et al., 2012). However, these indices are still calculated from the detrended phase with a fixed cutoff frequency, which can be affected by changes the Fresnel frequency due to changes in the ionospheric drift velocity. These studies indicate that the fundamental question still remains regarding the effect of ionospheric drift on the variation of the phase of GPS signal and the determination of the phase scintillation index. A recent study by Jayachandran et al. (2017) has shown that in the polar region both amplitude and phase scintillation raw time series and the spectra exhibit similar behaviors as expected.

In this paper, we present the first observational evidence on the relationship between the phase scintillation index and the plasma drift speed in the high-latitude noon sector based on the observations from the Canadian High Arctic Ionospheric Network (CHAIN) GPS receivers (Jayachandran et al., 2009) and the Super Dual Auroral Radar Network (SuperDARN) Kapuskasing (KAP) and Saskatoon (SAS) radar pair (Chisham et al., 2007; Greenwald et al., 1995).

2. Data and Method of Analysis

The scintillation data in this study are provided by GPS receivers of the CHAIN, which currently consist of 24 high data rate (50 Hz and 100 Hz sampling) GPS receivers distributed in the Canadian Arctic. For this particular study, we have used the 50 Hz data from the Novatel GSV4004B GPS receivers (at locations shown in Figure 1 by yellow stars). These receivers are capable of sampling only of 50 Hz. CHAIN GPS receivers offer a large spatial coverage in the high-latitude region. In this study, we focused on the 11:00–13:00 magnetic local time (MLT) sector over the 69° – 75° magnetic latitude (MLat) interval in the Northern Hemisphere, which is around the statistical cusp region in the Canadian sector and corresponds to 18:00–20:00 UT. Around this region, large variations in the plasma drift are often observed due to the dayside pulsed reconnection, particle precipitation, and associated ionospheric electrodynamics (e.g., Basu et al., 1994, 1998; Carlson et al., 2004, 2007; Moen et al., 2012, 2013; Oksavik et al., 2011, 2012; Zhang et al., 2008, 2010, 2011), making this an ideal region to study the effect of plasma drift on the GPS signal phase variations.

In order to quantify amplitude and phase variations, we have used the standard amplitude scintillation index (S_4) and phase scintillation index (σ_{ϕ}) with 1 min resolution. We have avoided GPS measurements lower than 20° elevation to mitigate multipath effects. For this study, both the carrier phase and amplitude are detrended using a sixth-order Butterworth filter with a fixed cutoff frequency of 0.1 Hz to remove long-term variations, which is often used by the receivers as well as many studies mentioned in section 1. This standard method has been adopted to show the issue experimentally, which was theoretically shown by Rino (1979) and quantitatively shown by Forte and Radicella (2002).

We also use plasma flow data from SuperDARN radars, which consist of more than 30 high-frequency radars with a wide coverage both in the Northern and Southern Hemispheres (Chisham et al., 2007). SuperDARN monitors the motion of field-aligned plasma irregularities in decameter-scale along line-of-sight directions of radar beams. The region of interest for this study is covered by the SuperDARN KAP and SAS radar pair. Based on line-of-sight Doppler measurements from these two radars, a plasma velocity can be obtained through the fitting process within the map potential technique (Ruohoniemi & Baker, 1998), which has a

Locations of CHAIN GISTMs and two of SuperDARN radars on 19:17 UT

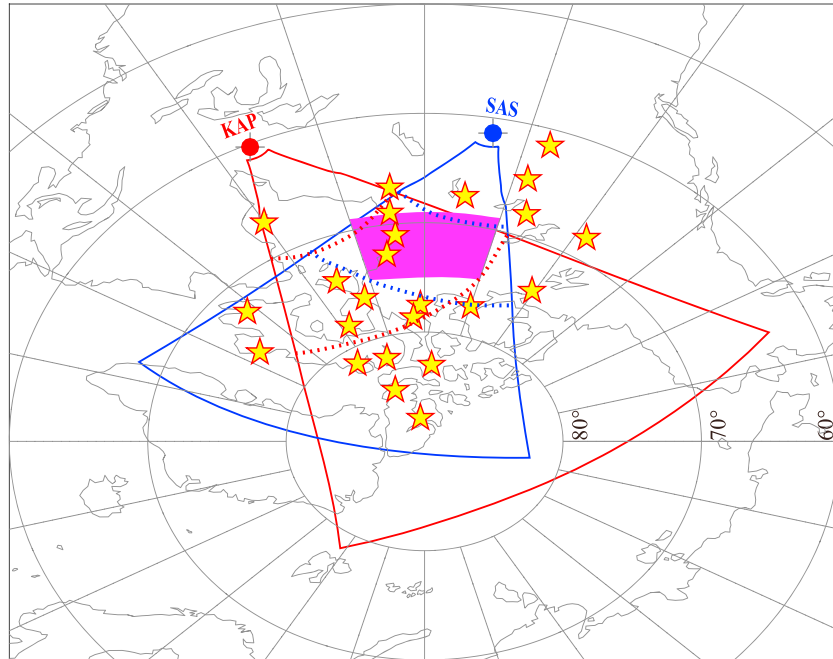


Figure 1. Map showing the locations of Canadian High Arctic Ionospheric Network (CHAIN) Global Positioning System receivers (yellow stars) and the field-of-view of Super Dual Auroral Radar Network (SuperDARN) Kapuskasing (KAP) and Saskatoon (SAS) radars in magnetic latitude/magnetic local time coordinate system with noon on the top down on the right at 19:17 UT. The specific observation zone is defined by two adjacent dotted curves, each corresponding to roughly the ionospheric F layer altitude. The region of interest in this study is highlighted by the magenta box covered by the two specific observation zones, which is in spatial range of 69° – 75° magnetic latitude and 11:00–13:00 magnetic local time during 18:00–20:00 UT interval.

time resolution of 2 min and a spatial resolution of 1° MLat \times 2° magnetic longitude under Altitude Adjustment Corrected Geomagnetic coordinates (herein and after).

Figure 1 shows an overview of the distributions of the CHAIN GPS receivers (marked with yellow stars) and the field-of-view of the SuperDARN KAP and SAS radars on MLat/MLT grid with noon top at 19:17 UT on 17 March 2015. The highlighted magenta region represents the region of 69° – 75° MLat and 11:00–13:00 MLT, which is referred as “the selected region” herein. This region is considered in this study for the following reasons: (1) This region is usually identified as the region of high plasma drift variability (Basu et al., 1994, 1998; Carlson et al., 2004, 2007; Moen et al., 2013; Oksavik et al., 2011, 2012; Zhang et al., 2008, 2010, 2011); (2) availability of the SuperDARN radar backscatter from both radars to obtain merged drift vectors; and (3) availability of a number of GPS receivers and multiple intersection raypaths in and around the region of interest.

3. Results

A selected example of a 2-D map of plasma flow together with maps of the amplitude and phase scintillation indices is shown in Figure 2. Each map is in MLat and MLT coordinates at 19:17 UT on 17 March 2015. During this period, a severe geomagnetic storm occurred that has been much studied. This storm condition provided us with a data of highly variable convection to illustrate the dependence of σ_{ϕ} on plasma flow. Figure 2 shows the plasma drift velocity, σ_{ϕ} and S_4 , respectively. In each panel, the sector with the magenta frame is the selected region we are considering for this study. In Figures 2b and 2c, the colored squares (including the gray) represent averaged scintillation indices in the spatial region of 1° MLat and 8 min in MLT. The adopted altitude of ionospheric pierce points of these indices is 350 km, roughly indicating the F_2 region of ionosphere. This particular method for projecting GPS scintillations has been adapted by Wang et al. (2016). For comparison with the 2 min resolution plasma drift data from radars, related scintillation data are taken

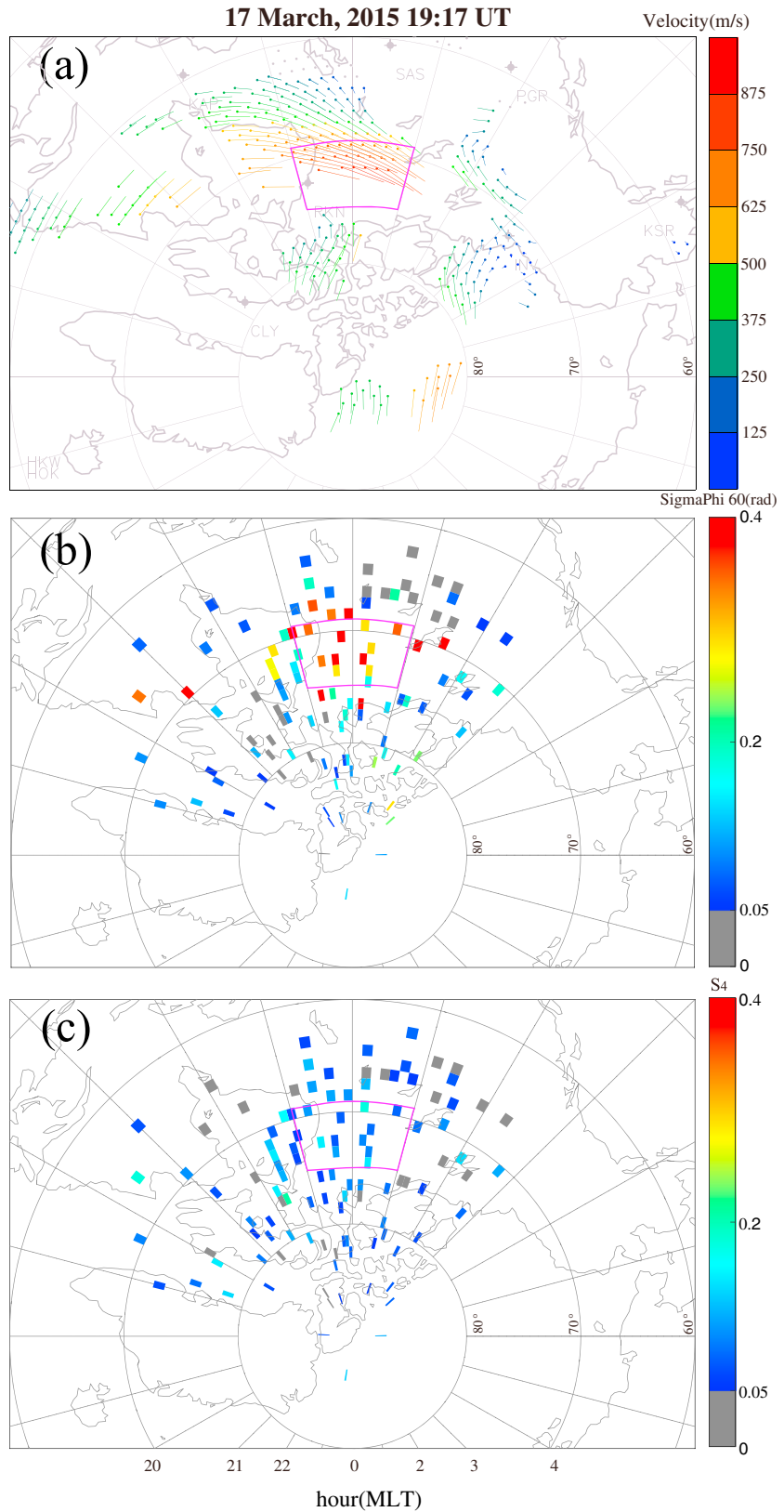


Figure 2. An example map of plasma drift vector (a) determined by Super Dual Auroral Radar Network Saskatoon-Kapusking radar pair, Global Positioning System phase (b) and amplitude (c) scintillation in magnetic local time-magnetic local time (MLT) coordinates. Noon is on the top at 19:17 UT on 17 March 2015.

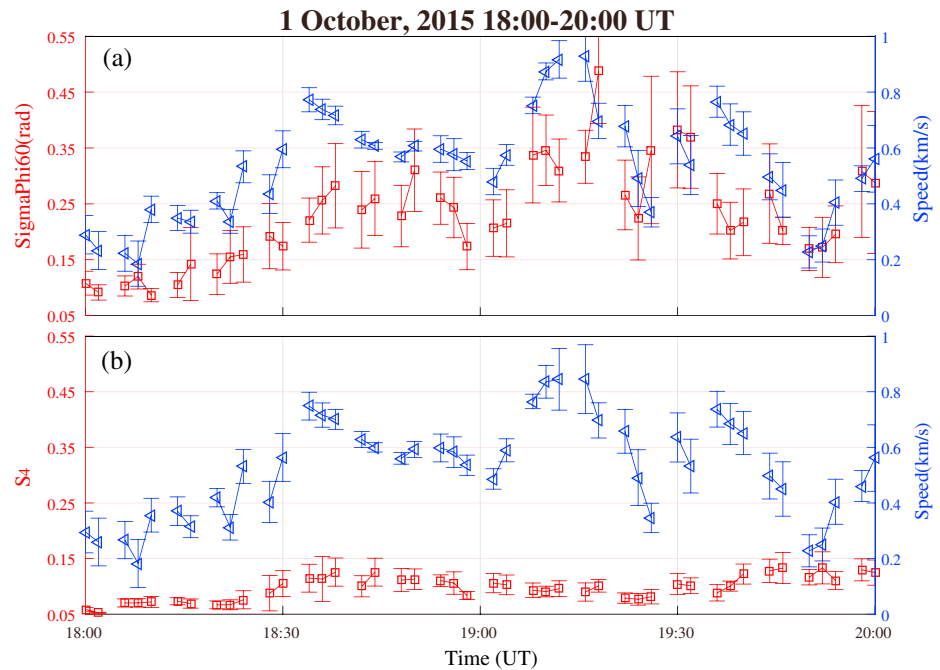


Figure 3. An example of time series of (a) average flow speed (blue line) and phase scintillation index (red line) and (b) average flow speed (blue line) and amplitude scintillation index (red line) in the region of interest (magenta box in Figure 1). Error bars are the standard deviations of each measurement. The time series is for the interval 18:00–20:00 UT on 1 October 2015.

at the middle time of each velocity interval. For example, when the radar measurements during the interval 19:16–19:18 UT used, the scintillation data at 19:17 UT will be taken. These figures show strong flows measured by SuperDARN radars in and around the selected region (marked by the box), while the corresponding σ_ϕ shows higher values in that region indicating strong phase variations ($\sigma_\phi > 0.4$ radians), whereas the corresponding S_4 shows very low values representing weak amplitude variations ($S_4 < 0.2$). Most of the published results (e.g., Doherty et al., 2003; Fremouw et al., 1978; Kintner et al., 2007; Oksavik et al., 2015; Pi et al., 2001) treated this as “phase without amplitude” scintillation. A closer look at the figure also reveals that there is a case outside the region of interest as well, which we did not consider for the study because of the criteria mentioned earlier.

Figure 3 shows an example of time series of averaged plasma drift speed, σ_ϕ , and S_4 for the period 18:00–20:00 UT on 1 October 2015 over the selected region. These data were extracted and averaged from the grids inside this region, which incorporates measurements of both scintillations and the velocity at a certain time. The top panel (Figure 3a) shows plasma drift speed and σ_ϕ variations, while the bottom panel (Figure 3b) shows plasma drift speed and S_4 variations. Error bars are standard deviations of these mean values over each averaging interval. The discontinuities of the lines in the time series represent data gaps. There is a high degree of correlation between plasma drift speed and scintillation indices with a higher degree of dependence of σ_ϕ (0.67) than S_4 (0.34) from Figure 3.

In order to further quantify the dependence of scintillation indices on plasma drift, a statistical study has been performed, using data from the region of interest (69°–75° MLat and 11:00–13:00 MLT) for a 3 year period from 2013 to 2015. We have binned the data in velocity bins of 5 m/s and averaged σ_ϕ and S_4 in each bin. Figure 4 shows the relationship between the plasma drift speed and scintillation indices. Figure 4a is for flow speed and σ_ϕ , and Figure 4b is for flow speed and S_4 . Each figure also shows the linear least squares fit with the correlation coefficient and the equation for the best fit based upon the average values in each bin. There is a high degree of correlation between plasma drift speed and both scintillation indices (correlation coefficient of 0.97 between σ_ϕ and plasma drift speed and correlation coefficient of 0.83 between S_4 and plasma drift speed). Note that the standard errors of correlation coefficient are 1.4×10^{-6} (σ_ϕ) and 9.4×10^{-6} (S_4).

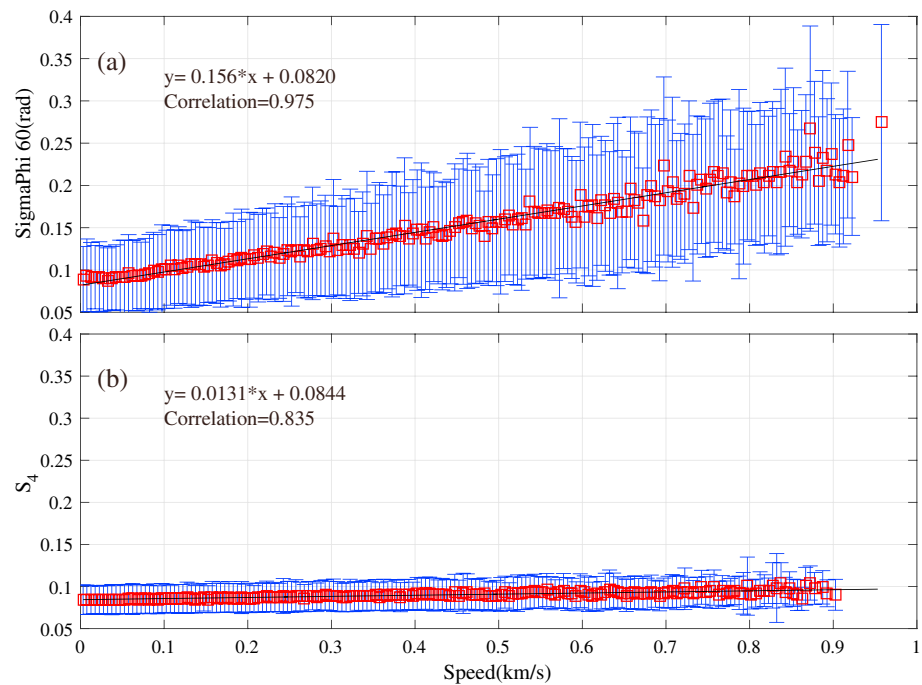


Figure 4. Scatterplot of the phase and amplitude scintillation with the flow speed. Flow speed is binned at 5 m/s bins. Box symbols are average scintillation indices in each bin, and error bars are standard deviation in each bin. Correlation coefficient of the averages and line of best fit to the averages are also shown in the figure.

However, the magnitude of the dependence on flow speed, as measured by the slope of the best fit, is 1 order of magnitude greater for σ_ϕ (0.16) when compared with S_4 (0.01). This is an important result and the first observational evidence that support the theoretical prediction of Rino (1979) and further quantification of Forte and Radicella (2002) that the phase variations/fluctuations exhibit a dependence on the relative drift velocity and the propagation geometry. Note that in this study only the magnitude of the plasma drift had been considered.

4. Discussion

Refractive effects (deterministic) on the phase of a transionospheric radio wave are well known and have a well-established relationship with electron density along the raypath and the frequency of a wave. These are caused by large-scale (larger than the Fresnel scale) electron density variations in the ionosphere. On the other hand, diffractive effects (stochastic) are stirred up by scales smaller than the Fresnel scale (e.g., Kintner et al., 2007). Fresnel scales are approximately 290 m for phase and 350 m for amplitude in L-band at a height of 350 km. Fresnel frequency is a crucial parameter when dealing with the GPS data. As mentioned above, refractive variations are expected to be caused mostly by large-scale structures (lower than the Fresnel frequency). These variations are typically assumed to be too low in frequency to be of importance in scintillation analysis and are ignored in many cases. However, if conditions are suitable (especially when the relative drift velocity is high), these refractive variations will be visible well past 0.1 Hz (often used as the cutoff frequency for detrending), frequencies typically associated with diffraction. Therefore, it is crucial to determine the Fresnel frequency accurately in order to eliminate refractive variations from the scintillation analysis. If it is not determined properly, one will be including refractive phase variations in the scintillation analysis and those will have higher phase scintillation index compared to amplitude scintillation index.

The results presented here clearly demonstrate a strong dependence of σ_ϕ , calculated using the standard approach, on the plasma drift speed. This dependence is possibly due to the increase in the difference between Fresnel frequency (due to the increase in relative drift speed which is proportional to the plasma drift) and the fixed cutoff frequency. As the relative drift speed increases, the Fresnel frequency increases and more refractive phase variation will be included in the scintillation analysis, which causes σ_ϕ to be

higher. If one were just looking at the scintillation indices, this would obviously explain the scenario of “phase without the amplitude” scintillation observed by many researchers (e.g., Doherty et al., 2003; Fremouw et al., 1978; Kintner et al., 2007; Oksavik et al., 2015; Pi et al., 2001). This also explains the observations of a larger occurrence percentage of phase scintillation when compared to amplitude scintillation in the high-latitude regions (Doherty et al., 2003; Prikrýl et al., 2013; Spogli et al., 2009).

Another possible explanation to the dependence of phase scintillation index on the convection speed is plasma instability mechanisms that in operation. There are two known plasma instability mechanisms that cause scintillations in the polar region. They are the gradient drift and Kelvin-Helmholtz instabilities (e.g., Basu et al., 1994, 1998; Carlson et al., 2007; De Franceschi et al., 2008; Moen et al., 2012, 2013; Oksavik et al., 2012). Gradient drift instability works on all density gradients along direction of the plasma flow, most effective at edges where the gradient is parallel to the flow, which is a convective instability with its nonlinear evolution (e.g., Keskinen & Ossakow, 1983; van der Meeren et al., 2014, and references therein). Kelvin-Helmholtz growth has a complicated dependence on the drift speed through the velocity shearing scale length. The lack of amplitude scintillation dependence on the drift speed strongly suggests that plasma instability mechanisms are not the cause of this dependence of phase scintillation index on the plasma drift speed.

One may also make the following argument since σ_ϕ is the standard deviation of the phase. Consider a diffraction pattern caused by irregularities and the raypath traverses this pattern at a constant velocity. Amplitude and phase scintillation will result, but phase scintillation will increase relative to zero velocity, and faster velocities will create phase scintillation from larger-scale functions in the diffraction pattern. In this case the absence of the amplitude scintillation will be the result of spatial filtering effect. In essence, this also boils down to the selection of the optimum detrending frequency (Fresnel frequency). If one detrends the signal with the correct frequency or under low drift speed (when 0.1 Hz is appropriate) phase and amplitude scintillation must appear together, dependent fundamentally on the diffraction/interference pattern caused by the irregularities as recently shown by Jayachandran et al. (2017).

As discussed above, the observed dependence can be explained more likely by a problem that the selection of the fixed cutoff frequency of 0.1 Hz for the high-latitude regions. This constant cutoff frequency of 0.1 Hz was first used by Fremouw et al. (1978) in their experiments and subsequently adapted for GPS for all latitude regions. In the nightside auroral region, the two fixed cutoff frequencies of 0.1 Hz and 0.3 Hz have been tested to estimate the effect of cutoff frequency on identifying the scintillations (Forte, 2005; van der Meeren et al., 2014). When the cutoff frequency was increased from 0.1 Hz to 0.3 Hz, phase fluctuations were found to be weaker still without amplitude scintillations. Recently, Mushini et al. (2012) have shown that proper treatment of the data leads to complete elimination of the “phase without amplitude” scintillation. Precise determination of the Fresnel frequency ergo the detrending cutoff frequency, one needs to use the geometry of the satellite track with respect to the plasma flow and the precise height of the ionospheric structure.

5. Conclusion

This paper presents the first evidence for the strong dependence of phase scintillation index (σ_ϕ) on the plasma drift in the noon sector of polar region. This observed dependence can and should be rectified by dynamical selection of the cutoff frequency in detrending the GPS data, using simultaneous and collocated plasma drift measurements. This dependence may also explain a higher occurrence of phase scintillation in the high-latitude region when compared to amplitude scintillation and the so-called phenomenon “phase without amplitude” scintillation. This paper also amplifies the importance of taking the utmost care in using the phase scintillation index in the high-latitude regions.

References

- Basu, S., Basu, S., Chaturvedi, P. K., & Bryant, C. M. (1994). Irregularity structures in the cusp/cleft and polar cap regions. *Radio Science*, 29(1), 195–207. <https://doi.org/10.1029/93RS01515>
- Basu, S., Weber, E. J., Bullett, T. W., Keskinen, M. J., MacKenzie, E., Doherty, P., et al. (1998). Characteristics of plasma structuring in the cusp/cleft region at Svalbard. *Radio Science*, 33(6), 1885–1899. <https://doi.org/10.1029/98RS01597>
- Beach, L. T. (2006). Perils of the GPS phase scintillation index (σ_ϕ). *Radio Science*, 41, RS5531. <https://doi.org/10.1029/2005RS003356>
- Carlson, H. C., Oksavik, K., Moen, J., & Pedersen, T. (2004). Ionospheric patch formation: Direct measurements of the origin of a polar cap patch. *Geophysical Research Letters*, 31, L08806. <https://doi.org/10.1029/2003GL018166>

Acknowledgments

This work in China is supported by the National Natural Science Foundation (grants 41574138, 41274149, and 41604139), the young top-notch talent program of the “National High-level personnel of special support program (Ten Thousand Talent Program),” and the Shandong Provincial Natural Science Foundation (grant JQ201412) and the Chinese meridian project. All the GPS data used in this work were provided by the Canadian High Arctic Ionospheric Network (CHAIN); the official website is <http://chain.physics.unb.ca/chain/>. Infrastructure funding for CHAIN was provided by the Canada Foundation for Innovation (CFI) and the New Brunswick Innovation Foundation (NBIF). CHAIN and its operation are conducted in collaboration with the Canadian Space Agency (CSA). Science funding is provided by the Natural Sciences and Engineering Research Council of Canada (NSERC). J. Moen is supported by the Research Council of Norway grant 230996. M. Lester acknowledges support from STFC grant ST/K001000/1 and NERC grant NE/K011766/1. We greatly appreciate the Physics department of University of New Brunswick for establishing and running CHAIN and sharing scintillation data through database <http://chain.physics.unb.ca/chain/pages/gps/>. We also sincerely acknowledge Virginia Tech. for providing SuperDARN radar data through website (<http://vt.superdarn.org/tiki-index.php>). SuperDARN is a collection of radars funded by national scientific funding agencies of Australia, Canada, China, France, Japan, South Africa, UK, and United States. The Kapuskasing HF radar is operating by Virginia Tech., and the Saskatoon HF radar is maintained by University of Saskatchewan. The authors also wish to thank the International Space Science Institute in Beijing (ISSI-BJ) for supporting and hosting the meeting of the International Team on “Multiple-instrument observations and simulations of the dynamical processes associated with polar cap patches/aurora and their associated scintillations,” during which the discussions leading/contributing to this publication were held.

- Carlson, H. C., Pedersen, T., Basu, S., Keskinen, M., & Moen, J. (2007). Case for a new process, not mechanism, for cusp irregularity production. *Journal of Geophysical Research*, *112*, A11304. <https://doi.org/10.1029/2007JA012384>
- Chisham, G., Lester, M., Milan, S. E., Freeman, M. P., Bristow, W. A., Grocott, A., et al. (2007). A decade of the Super Dual Auroral Radar Network (SuperDARN): Scientific achievements, new techniques and future directions. *Surveys in Geophysics*, *28*(1), 33–109. <https://doi.org/10.1007/s10712-007-9017-8>
- De Franceschi, G., Alfonsi, L., Romano, V., Aquino, M., Dodson, A., Mitchell, C. N., et al. (2008). Dynamics of high-latitude patches and associated small-scale irregularities during the October and November 2003 storms. *Journal of Atmospheric and Solar - Terrestrial Physics*, *70*, 879–888. <https://doi.org/10.1016/j.jastp.2007.05.018>
- Doherty, P. H., Delay, S. H., Valladares, C. E., & Klobuchar, J. A. (2003). Ionospheric scintillation effects in the equatorial and auroral regions. *Journal of the Institute of Navigation*, *50*(4), Winter 2003–2004, 235–246.
- Forté, B. (2005). Optimum detrending of raw GPS data for scintillation measurements at auroral latitudes. *Journal of Atmospheric and Terrestrial Physics*, *67*, 1100–1109. <https://doi.org/10.1016/j.jastp.2005.01.011>
- Forté, B., & Radicella, S. M. (2002). Problems in data treatment for ionospheric scintillation measurements. *Radio Science*, *37*(6), 1096. <https://doi.org/10.1029/2001RS002508>
- Fremouw, E. J., Leadabrand, R. L., Livingston, R. C., Cousins, M. D., Rino, C. L., Fair, B. C., & Long, R. A. (1978). Early results from the DNA Wideband satellite experiment: Complex signal analysis. *Radio Science*, *13*(1), 167–187.
- Greenwald, R. A., Bristow, W. A., Sofko, G. J., Senior, C., Cerisier, J. C., & Szabo, A. (1995). Super dual auroral radar network radar imaging of dayside high-latitude convection under northward interplanetary magnetic field: Toward resolving the distorted two-cell versus multicell controversy. *Journal of Geophysical Research*, *100*, 19661. <https://doi.org/10.1029/95JA01215>
- Jayachandran, P. T., Hamza, A. M., Hosokawa, K., Mezaoui, H., & Shiokawa, K. (2017). GPS amplitude and phase scintillation associated with polar cap auroral forms. *Journal of Atmospheric and Terrestrial Physics*, *164*, 185–191. <https://doi.org/10.1016/j.jastp.2017.08.030>
- Jayachandran, P. T., Langley, R. B., MacDougall, J. W., Mushini, S. C., Pokhotelov, D., Hamza, A. M., et al. (2009). Canadian High Arctic Ionospheric Network (CHAIN). *Radio Science*, *44*, RS0A03. <https://doi.org/10.1029/2008RS0040046>
- Jin, Y., Moen, J. I., & Miloch, W. J. (2015). On the collocation of the cusp aurora and the GPS phase scintillation: A statistical study. *Journal of Geophysical Research*, *120*, 9176–9191. <https://doi.org/10.1002/2015JA021449>
- Keskinen, M. J., & Ossakow, S. L. (1983). Theories of high-latitude ionospheric irregularities: A review. *Radio Science*, *18*(6), 1077–1091.
- Kintner, P. M., Ledvina, B. M., & de Paula, E. R. (2007). GPS and ionospheric scintillations. *Space Weather*, *5*, S09003. <https://doi.org/10.1029/2006SW000260>
- Kintner, P. M., Ledvina, B. M., de Paula, E. R., & Kantor, I. J. (2004). Size, shape, orientation, speed, and duration of GPS equatorial anomaly scintillations. *Radio Science*, *39*, RS2012. <https://doi.org/10.1029/2003RS002878>
- Li, G., Ning, B., Hu, L., Liu, L., Yue, X., Wan, W., et al. (2010). Longitudinal development of low-latitude ionospheric irregularities during the geomagnetic storms of July 2004. *Journal of Geophysical Research*, *115*, A04304. <https://doi.org/10.1029/2009JA014830>
- MacDougall, J. W., & Jayachandran, P. T. (2001). Polar cap convection relationships with solar wind. *Radio Science*, *36*(6), 1869–1880.
- Materassi, M., Alfonsi, L., De Franceschi, G., & Romano, V., Mitchell, C., Spalla P. (2009). Detrend effect on the scalograms of GPS power scintillation. *Advances in Space Research*, *43*(11), 1740–1748. <https://doi.org/10.1016/j.asr.2008.01.023>
- Materassi, M., & Mitchell, C. N. (2007). Wavelet analysis of GPS amplitude scintillation: A case study. *Radio Science*, *42*, RS1004. <https://doi.org/10.1029/2005RS003415>
- Moen, J., Oksavik, K., Abe, T., Lester, M., Saito, Y., Bekkeng, T. A., & Jacobsen, K. S. (2012). First in-situ measurements of HF radar echoing targets. *Geophysical Research Letters*, *39*, L07104. <https://doi.org/10.1029/2012GL051407>
- Moen, J., Oksavik, K., Alfonsi, L., Daabakk, Y., Romano, V., & Spogli, L. (2013). Space weather challenges of the polar cap ionosphere. *Journal of Space Weather and Space Climate*, *3*, A02. <https://doi.org/10.1051/SWSC/2013025>
- Mushini, S. C., Jayachandran, P. T., Langley, R. B., MacDougall, J. W., & Pokhotelov, D. (2012). Improved amplitude- and phase-scintillation indices derived from wavelet detrended high-latitude GPS data. *GPS Solutions*, *16*(3), 363–373. <https://doi.org/10.1007/s10291-011-0238-4>
- Oksavik, K., Moen, J., Lester, M., Bekkeng, T. A., & Bekkeng, J. K. (2012). In situ measurements of plasma irregularity growth in the cusp ionosphere. *Journal of Geophysical Research: Space Physics*, *117*, A11301. <https://doi.org/10.1029/2012JA017835>
- Oksavik, K., Moen, J. I., Rekaa, E. H., Carlson, H. C., & Lester, M. (2011). Reversed flow events in the cusp ionosphere detected by SuperDARN HF radars. *Journal of Geophysical Research: Space Physics*, *116*, A12303. <https://doi.org/10.1029/2011JA016788>
- Oksavik, K., van der Meer, C., Lorentzen, D. A., Baddeley, L. J., & Moen, J. (2015). Scintillation and loss of signal lock from poleward moving auroral forms in the cusp ionosphere. *Journal of Geophysical Research: Space Physics*, *120*, 9161–9175. <https://doi.org/10.1002/2015JA021528>
- Pi, X., Boulat, B., Mannucci, A. J., Reyes, M., & Stowers, D. (2001). *Ionospheric scintillations measured using GPS receivers during the current solar maximum*. Boston: International Beacon Satellite Symposium.
- Prikryl, P., Jayachandran, P., Mushini, S. C., & Richardson, I. G. (2014). High-latitude GPS phase scintillation and cycle slips during high-speed solar wind streams and interplanetary coronal mass ejections: A superposed epoch analysis. *Earth, Planets and Space*, *66*(1), 62. <https://doi.org/10.1186/1880-5981-66-62>
- Prikryl, P., Jayachandran, P. T., Mushini, S. C., Pokhotelov, D., MacDougall, J. W., Donovan, E., et al. (2010). GPS TEC, scintillation and cycle slips observed at high latitudes during solar minimum. *Annales de Geophysique*, *28*(6), 1307–1316. <https://doi.org/10.5194/angeo-28-1307-2010>
- Prikryl, P., Jayachandran, P. T., Mushini, S. C., & Richardson, I. G. (2012). Toward the probabilistic forecasting of high-latitude GPS phase scintillation. *Space Weather*, *10*, S08005. <https://doi.org/10.1029/2012SW000800>
- Prikryl, P., Sreeja, P. V., Aquino, M., & Jayachandran, P. T. (2013). Probabilistic forecasting of ionospheric scintillation and GNSS receiver signal tracking performance at high latitudes. *Annales de Geophysique*, *56*, R0222. <https://doi.org/10.4401/ag-6219>
- Rino, C. L. (1979). A power law phase screen model for ionospheric scintillation, 1. Weak scatter. *Radio Science*, *14*(6), 1135–1145.
- Ruohoniemi, J. M., & Baker, K. B. (1998). Large-scale imaging of high-latitude convection with SuperDARN HF radar observations. *Journal of Geophysical Research: Space Physics*, *103*(A9), 20,797–20,811. <https://doi.org/10.1029/98JA01288>
- Spogli, L., Alfonsi, L., De Franceschi, G., Romano, V., Aquino, M. H. O., & Dodson, A. (2009). Climatology of GPS ionospheric scintillations over high and mid-latitude European regions. *Annales de Geophysique*, *27*(9), 3429–3437. <https://doi.org/10.5194/angeo-27-3429-2009>
- van der Meer, C., Oksavik, K., Lorentzen, D., Moen, J. I., & Romano, V. (2014). GPS scintillation and irregularities at the front of an ionization tongue in the nightside polar ionosphere. *Journal of Geophysical Research: Space Physics*, *119*, 8624–8636. <https://doi.org/10.1002/2014JA020114>
- Van Dierendonck, A. J., & Arbesser-Rastburg, B. (2004). Measuring ionospheric scintillation in the equatorial region over Africa, including measurements from SBAS geostationary satellite signals, *Proc. ION GNSS 17th technical meeting*.

- Van Dierendonck, A. J., Klobuchar, J. A., & Hua, Q. (1993). Ionospheric scintillation monitoring using commercial single frequency C/A code receivers, paper presented at ION GPS-93, Inst. of Navigat., Arlington, Va.
- Wang, Y., Zhang, Q. H., Jayachandran, P. T., Lockwood, M., Zhang, S. R., Moen, J., et al. (2016). A comparison between large-scale irregularities and scintillations in the polar ionosphere. *Geophysical Research Letters*, *43*, 4790–4798. <https://doi.org/10.1002/2016GL069230>
- Zhang, Q. H., Dunlop, M. W., Liu, R. Y., Yang, H. G., Hu, H. Q., Zhang, B. C., et al. (2011). Coordinated Cluster/Double star and ground-based observations of dayside reconnection signatures on 11 February 2004. *Annales de Geophysique*, *29*(10), 1827–1847. <https://doi.org/10.5194/angeo-29-1827-2011>
- Zhang, Q. H., Dunlop, M. W., Lockwood, M., Liu, R. Y., Hu, H. Q., Yang, H. G., et al. (2010). Simultaneous observations of reconnection pulses at Cluster and their effects on the cusp aurora observed at the Chinese Yellow River Station. *Journal of Geophysical Research*, *115*, A10237. <https://doi.org/10.1029/2010JA015526>
- Zhang, Q. H., Liu, R. Y., Dunlop, M. W., Huang, J. Y., Hu, H. Q., Lester, M., et al. (2008). Simultaneous tracking of reconnected flux tubes: Cluster and conjugate SuperDARN observations on 1 April 2004. *Annales de Geophysique*, *26*(6), 1545–1557. <https://doi.org/10.5194/angeo-26-1545-2008>